Hindawi Publishing Corporation
Journal of Nanomaterials
Volume 2012, Article ID 413542, 6 pages
doi:10.1155/2012/413542

Research Article

Degradation of Semiconductor Manufacturing Wastewater by Using a Novel Magnetic Composite TiO_2/Fe_3O_4 Photoreactor Design

Chen-Yu Chang[1] and Yung-Hsu Hsieh[2]

[1] *Center of General Education, National Taitung College, 889 Jhengci N. Rdoa, Taitung City 95045, Taiwan*
[2] *Department of Environmental Engineering, National Chung Hsing University, 250 Kuo-Kung Road, Taichung City 402, Taiwan*

Correspondence should be addressed to Chen-Yu Chang, cyc1136@ntc.edu.tw

Received 13 February 2012; Revised 25 April 2012; Accepted 26 April 2012

Academic Editor: Jiaguo Yu

The purpose of this research is to develop a photocatalytic TiO_2 that can be activated by visible light and can be conveniently recollected for reusing. This research synthesizes the 20 to 40 nm TiO_2/Fe_3O_4 particles with magnetization of 5.8 emu/g using the modified sol-gel method followed by 500°C calcinations. The experiment verified that visible fluorescent light (VFL, contains no UV-A) could activate the photocatalytic activity of TiO_2/Fe_3O_4 particles as did ultraviolet A light (UV-A, 360 nm). Regular magnets can be used to separate TiO_2/Fe_3O_4 particles from solution. The results indicate that VFL-sirradiated TiO_2/Fe_3O_4 particles could decompose isopropanol (IPA) in the absence of UV-A and the issue of TiO_2/Fe_3O_4 recollection from water for reusing is also resolved.

1. Introduction

In the typical semiconductor manufacturing processes, a large amount of IPA is used for wafer cleaning. The wafer cleaning processes invariably generate a large quantity of wastewater that contains refractory and complex organic compounds. Not only do these organic compounds pose direct or indirect harm to the liver, kidney, central nervous system, and skin, some of them have already been verified as carcinogen, teratogenic agent, and gene mutagen for humans. Traditional wastewater treatment approaches involving physical-chemical decomposition or microorganisms have shown only limited efficiencies [1]. Many advanced oxidation processes (AOPs) have been extensively utilized for the decomposition of hazardous or recalcitrant pollutants in the environment. In recent years, TiO_2 has attracted much attention because of the low price and steady and high photocatalytic activation [1–4]. However, requirement of using UV light to activate TiO_2 photocatalyst and difficultly to recover the photocatalyst are still major limitationly for degradation of environmental pollutants [5, 6]. There are many types of conventional methods to modify quality of photocatalyst. One of them is TiO_2 photocatalyst doped by the transition metal [7–22]. It makes the defect of the structure of TiO_2 and produces the lower energy gap. Therefore, just less energy reacts with O_2 and H_2O in the environment to form the excited electron and holes. As a consequence, the absorbed spectrum of TiO_2 can shift into the region of visible light. V, Fe, Cr, Ni, Cu, and other transition metals are well-known to be doped into TiO_2 thin film to shift the band gap to visible light. Producing visible-light-activated TiO_2 powder for easy recovery can be beneficial. Iron enhances TiO_2 visible light absorption and thus increases its photocatalytic activity. Previous researches have reported that iron-based nanoparticles have been superparamagnetic [1, 18, 23, 24] and have been coated with organic polymers such as porphyrin and other dyes [6, 25, 26] or other inorganic elements such as N and H [27–29] and other methods [29, 30]. This research uses sol-gel method to add Fe_3O_4 during TiO_2 synthesis and then uses visible-light-irradiated TiO_2/Fe_3O_4 to conduct photodegradation effect on IPA. The photodegradation efficiency of IPA and

the recovery rate of photocatalyst will be also evaluated in this study.

2. Experimental/Materials and Methods

2.1. Preparation of Photocatalyst. In this study, the TiO_2/Fe_3O_4 complex was prepared using the modified sol-gel method [4]. The sol-gel process is one of the versatile methods to prepare high-pure and nanosize materials shaped as powders or coatings. This approach does not need complicated instruments such as chemical vapor deposition. It provides a simple and easy method to synthesize nanosize photocatalysts. First, soluble TiO_2 precursor powder was prepared using a mixture of tetraisopropyl orthotitanate ($Ti(OC_3H_7)_4$) (TTIP, >98%, Merck Co.), 2-propanol (>99.7%, JT. Baker), and acetic acid (>99.9%, JT. Baker). Then, the mixed solutions were stirred for 24 h and dried at 105°C followed by 150°C for 1 h, respectively. The dried gel was then pulverized into powder and calcinated in the high-temperature oven. The parameters employed to control the preparation of the catalyst include 2-propanol, acetic acid (TTIP was fixed), calcinations time, and calcinations temperature. The orthogonal arrays in the design of the experimental method proposed by Taguchi were adopted to conduct the multiple-factor experiment. Second, the above-prepared TiO_2 powder was directly mixed with iron oxide (Fe_3O_4, >98%, Aldrich) and Fe_3O_4/TiO_2 at the designed molar ratio of 0.1. Then, the mixed solutions were stirred for 1 h and dried at 105°C for 1 h. The conversion rate of IPA in this experiment was employed to identify the optimal conditions for assembly. The reactor containing TiO_2/Fe_3O_4 complexes was irradiated with 419 nm fluorescent lamps to undergo the batch photocatalytic degradation experiment.

2.2. Photoelectrocatalytic Procedure. The liquid-phase photoelectrocatalytic system consisted of 16 VFLs (Rayonet Model RPR 100 Photochemistry Reactor, the Southern New England Ultraviolet Company, fluorescent lamps λ_{max} = 419 nm, intensity = 724 lx), a completely mixing reactor, and an air compressor for aeration and stirring use, and a peristaltic pump was used to draw sample into the reactor for the continuous refluxing batch experiments and the flow rate controlled at 300 mL min^{-1}. The apparatus is illustrated in Figure 1. The experiment used the batch reaction system with the aqueous sample of 850 mL, and the controlled parameters were pH values and the amount of photocatalyst. A gas chromatography equipped with flame ionization detector (GC-FID; Agilent Co., Model HP6890 Series) and chromatography column (60 m × 0.32 mm × 0.5 μm, Agilent HP-INNOWax) were employed to determine the concentration of IPA. Total organic carbon instruments (TOC; Shimadzu, Japan, Model TOC-VCSN) were employed for the analysis of the experiment to investigate the variations of the residual rates and the mineralization rates under the parameters described above. Besides, all the other chemicals were of either analytical or reagent grade. The deionized water (≥18 MΩcm^{-1}) used for preparing the chemical solutions was processed by the Milli-Ultrapure R/O System (Millipore, USA) to ensure the quality of the prepared solution.

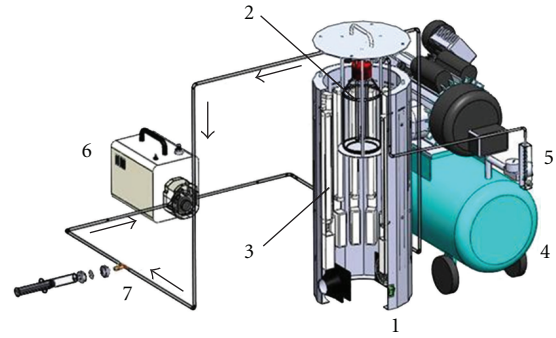

(1) Photocatalystic chamber
(2) Reactor
(3) Visible light
(4) Air compressor
(5) Mass flow meter
(6) Peristaltic pump
(7) Sampling syringe

Figure 1: Schematic diagram of continuous photocatalytic degradation system.

3. Results and Discussion

3.1. Optimal Preparation of Photocatalysts Using Taguchi Method. The controlling factors, which include 2-propanol (0.08, 0.16, and 0.32 mol), acetic acid (0.08, 0.16, and 0.32 mol), calcinations temperature (400, 500, and 600°C), and calcinations time (90, 120, and 180 min), were chosen according to the work of Cheng et al. [4]. The orthogonal arrays in the experimental design proposed by Zhang [31] were adopted to conduct the multiple-factor experiment and obtain the best combination of conditions for experimental photocatalytic conversion of IPA. The four parameters of various levels yield 9 different combinations as summarized in the L_9 orthogonal array table. Different photocatalysts were prepared according to different combinations of controlling factors for conducting the heterogeneous photocatalytic reactions to obtain the conversion rates of IPA. The IPA conversion rates thus obtained were then statistically analyzed by the F test to determine the significance and variability of each factor. The result showed that, among the factors, calcinations temperature had the greatest effect on conversion rate of IPA in the photocatalysis system (42.06%), followed by calcinations time (27.14%), the amount of 2-propanol (14.86%), and, finally, the amount of acetic acid (14.67%). In general, the effect of calcination temperature was more significant due to its function in removing impurities and increasing crystal strength. Table 1 shows the contributions and major effects of different parameters. The optimal preparation condition of TiO_2 catalyst was achieved under water 2-propanol of 0.08 mol, acetic acid of 0.32 mol (i.e., TTIP/2-proanol/acetic acid with a molar ratio of 1 : 2 : 8), calcinations temperature of 500°C, and calcinations time of 90 min. The TiO_2 was prepared at the above optimal experimental conditions. Then, the above prepared TiO_2 powder was directly mixed with Fe_3O_4 and Fe_3O_4/TiO_2 at the designed molar ratio of 0.1, and the mixed solutions were stirred for 1 h and dried at 105°C for 1 h. The solid was calcinated in an atmospheric oven heated to 200°C at

Table 1: Response of parameters in L_9 table.

Factors	2-propanol (mol)	Acetic acid (mol)	Calcination temperature (°C)	Calcination time (min)
Level 1	61.89	48.52	52.98	67.51
Level 2	47.54	62.11	36.67	40. 64
Level 3	59.19	58.03	78.64	60.08
Main effect	14.86	14.67	42.06	27.14

Figure 2: The appearance of TiO_2 particles.

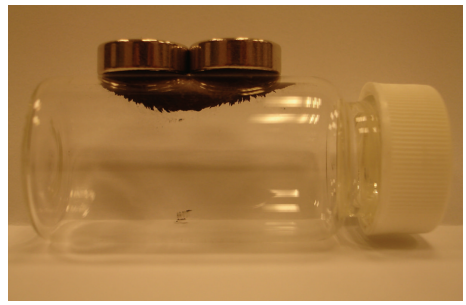

Figure 3: The appearance of Fe_3O_4 particles.

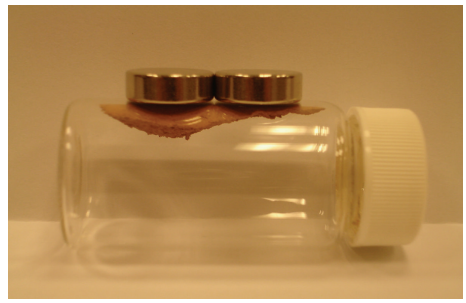

Figure 4: The appearance of TiO_2/Fe_3O_4 particles.

the rate of 5°C/min, held for 1 h and reheated to 500°C at the rate of 5°C/min, and then held for another 3 h. The solid was grounded into powder, washed with distilled water, and then dried at 60°C.

3.2. Properties Analysis of Photocatalysts. The photocatalyst prepared by the modified sol-gel method under the optimal conditions described above and the magnetism was tested and is shown in Figures 2, 3, and 4. As can be seen, the pure Fe_3O_4 particles and TiO_2/Fe_3O_4 composite catalyst also had good magenetism. The magnetization curve of TiO_2/Fe_3O_4 composite catalyst was measured with Superconducting Quantum Interference Device Magnetometer (SQUID; SQUID-PMS5, Quantum Design Corp.), and Figure 5 illustrates the saturation magnetization intensity of TiO_2/Fe_3O_4 composite catalyst was 5.8 emu/g. The field-emission scanning electron micrographs (FE-SEM, JSM-6700F, JEOL, Japan) of TiO_2/Fe_3O_4 composite catalyst were shown in Figure 6, and they clearly displayed that the particle was little irregular and the size was about 20–40 nm. Anatase TiO_2 containing Fe_3O_4 was obtained and analyzed by the X-ray diffractometer (XRD) and compared with the JCPDS database (no. 84-1286 and 89-4319) (Figure 7). The X-ray diffractometer (XRD, MAC MXTIII) was used to examine the crystals form.

3.3. Adsorption Effect. In this study, the adsorption ability of the TiO_2/Fe_3O_4 composite catalyst has been studied at varied pH (4, 7, and 10) with 30 mg L^{-1} IPA without any irradiation at temperature of 25°C in the reaction chamber for 240 minutes. The adsorption ability for the TiO_2/Fe_3O_4 composite catalyst was weak under alkaline and neutral conditions but not significantly different. Because all of the adsorption rates were less than 1%, the effect of adsorption was not taken into consideration in the following experiments, which did not affect the interpretation of the data acquired.

3.4. Photoelectrocatalytic Tests. Because the photolytic efficiency of UV irradiation treated with IPA was less than 2% in 3 replicates test, therefore the part experiment was not taken into comparing in the subsequent experiments. The photoactivity indicator of the TiO_2/Fe_3O_4 composite catalyst was investigated by the conversion rate of IPA. The 2.0 g TiO_2/Fe_3O_4 composite catalyst was used to react with 30 mg L^{-1} IPA under 3.0 mW cm^{-2}, 365 nm UV light (UV-A), 724 lx VFL at pH 7 for 240 min. The results are illustrated in Figure 8, and the destruction removal efficiency (DRE) of the TiO_2/Fe_3O_4 composite catalyst on the conversion of IPA was higher than the TiO_2 catalyst alone. Evidence reveals that the system of the TiO_2/Fe_3O_4 complexes has significantly high efficiency of photocatalytic degradation than TiO_2 only.

From the experimental data, we could find and understand that the TiO_2 and TiO_2/Fe_3O_4 composites had good performance under UV irradiation because UV light was with higher energy, but this experiment verified that visible fluorescent light could activate the photocatalytic activity of TiO_2/Fe_3O_4 particles as did ultraviolet A light. The result showed that the TiO_2/Fe_3O_4 composite catalyst also had good destruction rate for IPA under visible light, and this evidence revealed that the system of the TiO_2/Fe_3O_4 composite catalyst could be used to treat organic pollutants in practical wastewater treatment factories.

3.5. pH Effect. Although there was no significant variation of adsorption experiments under different pH values, there

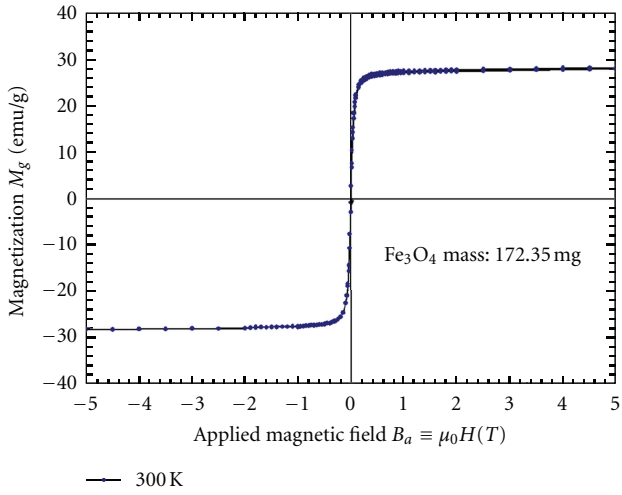

Figure 5: The SQUID analysis of TiO_2/Fe_3O_4 particles.

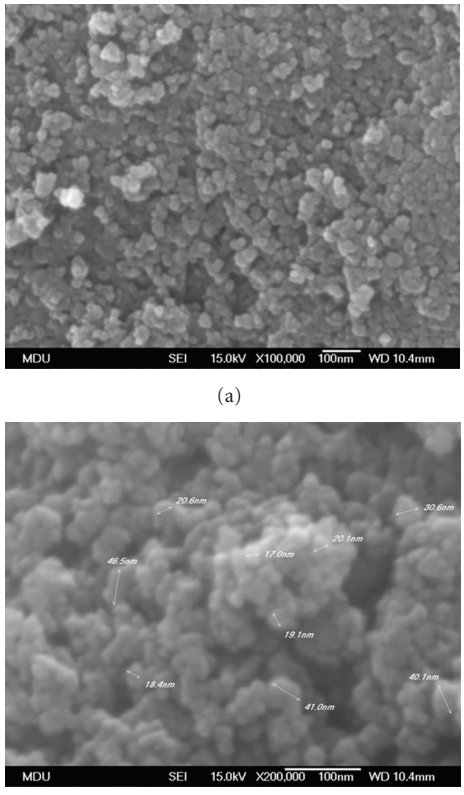

Figure 6: The SEM image of TiO_2/Fe_3O_4 particles.

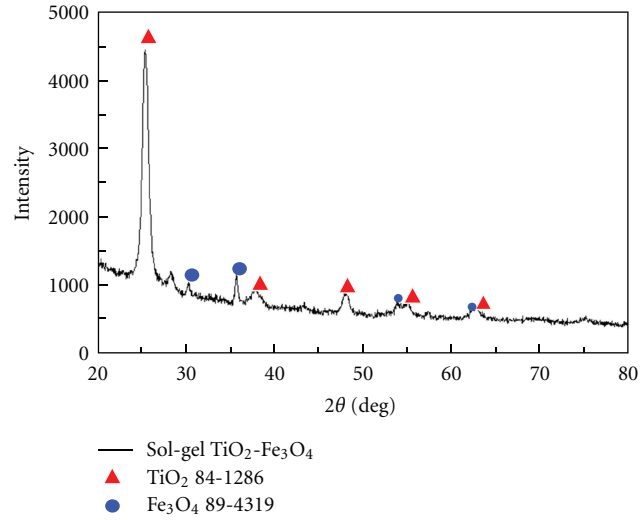

Figure 7: The X-ray diffraction spectrum of TiO_2/Fe_3O_4.

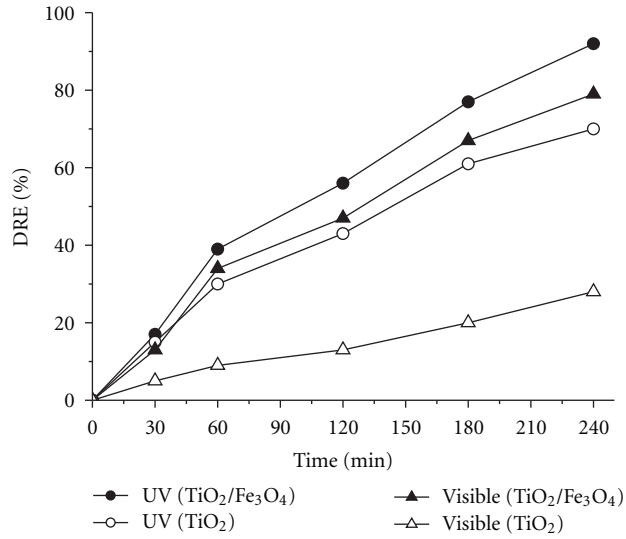

Figure 8: Comparison of the effect of TiO_2/Fe_3O_4 catalyst on the DRE of IPA under the UV-A and VFL irradiation.

were obvious variations in the photocatalytic reactions. In general, the yield of hydroxyl radicals in the photocatalytic reaction increases with increasing pH of the aqueous solution. However, the distribution ratios of the intermediates produced in the solution were directly related to the pH values. Moreover, the pH value alters the electrical behavior on the surface of the photocatalyst leading to changes in the absorption and desorption properties and capabilities of the intermediates produced by the catalyst. Therefore, the control of pH during the operation had significant impact on the efficiency of the overall treatment.

The pH_{zpc} value of TiO_2 is 6.4. Therefore, the TiO_2 surface carries a positive charge at pH below 6.4. However, more and more oxygen ions dissociate from the TiO_2 surface at pH above 6.4, causing a negative charge to develop on the catalyst surface. The substances formerly attached to the catalyst surface as a result of electrostatic adsorption begin to leave the catalyst under the influence of electric repulsion between the substances and the catalyst, thus lowering the oxidation/reduction rate of the reactants. Therefore, the ionic reactants are more affected by the pH of the environment due to electrostatic interaction. Figure 9 illustrates the destruction removal efficiency of IPA under the VFL irradiation for 240 minutes of photocatalytic reaction. As can

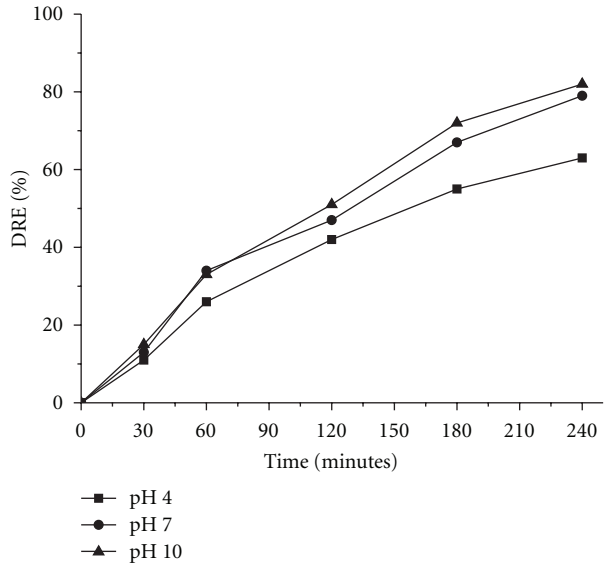

Figure 9: Destruction removal efficiency of IPA at different pH. (VFL, 2 g TiO_2/Fe_3O_4 catalyst, and IPA of 30 mg L^{-1}).

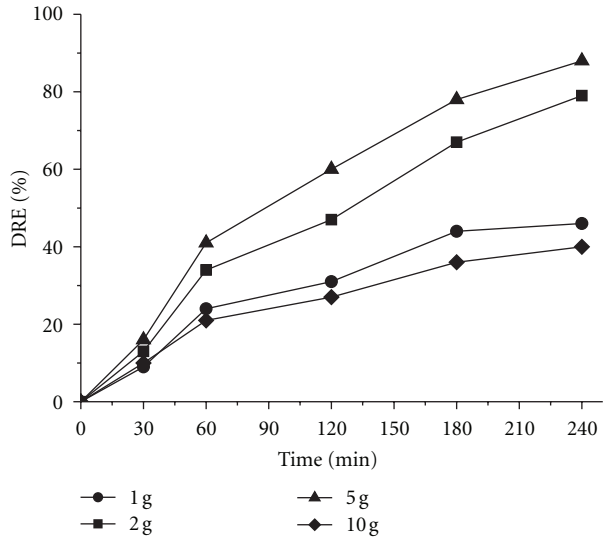

Figure 10: Destruction removal efficiency of IPA at different amount of photocatalysts. (VFL, pH of 7 and IPA of 30 mg L^{-1}).

be seen, the removal rate of IPA was higher under basic conditions, and the result coincided with previous studies [32].

3.6. Effect of Addition of Photocatalyst. The objective of the present study was to identify the optimal quantity of the TiO_2/Fe_3O_4 composite catalyst added according to economic consideration. This part of the experiment was carried out under the following conditions: initial IPA concentration of 30 mg L^{-1}, pH 7, temperature of 25°C, and VFL for 240 min. The variations in DRE thus obtained are illustrated in Figure 10. As can be seen, when the photocatalyst added was increased from 1 g to 5 g, the DRE was improved from

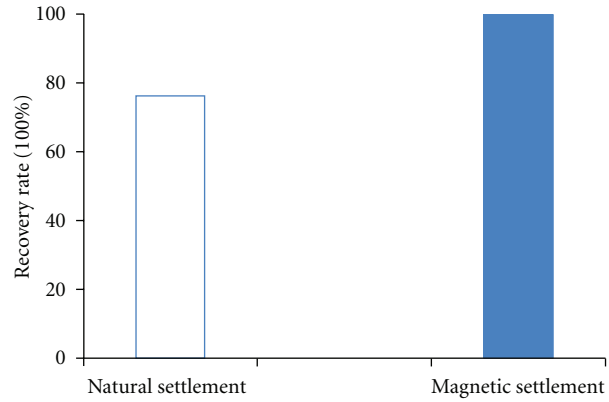

Figure 11: Recovery of TiO_2/Fe_3O_4 (3 g TiO_2/Fe_3O_4 under 3 minutes settling time).

46% to 88%. However, when the amount of the TiO_2/Fe_3O_4 composite catalyst added was increased from 5 g to 10 g, the DRE was reduced. It was speculated that excessive amount of the TiO_2/Fe_3O_4 photocatalyst added to the solution caused shielding of the light. Thus, both the light path and amount of TiO_2/Fe_3O_4 photocatalyst available for visible light irradiation were reduced, resulting in a decrease in overall treatment efficiency. At the same time, the recovery rate of photocatalyst could reach to 99.8% as we recollected easily from recycled water using magnet (shown in Figure 11). It is also illustrated that the system of TiO_2/Fe_3O_4 has significant efficiency of photodegradation under visible light irradiation and can be used and recycled in the practical wastewater treatment factories in the future.

4. Conclusions

Various dopants have been used for TiO_2 to absorb visible light. Fe_3O_4 was chosen and added during the preparation of TiO_2 photocatalystsusing sol-gel method that made TiO_2 photocatalytic activity be activated by visible light. In this study, the synthesized TiO_2/Fe_3O_4 can be activated by irradiation of UV-A and VFL. No significant photocatalytic activity was lost after being recollected from water using magnet for reusing. TiO_2/Fe_3O_4 also demonstrated the DRE of IPA under VFL and resolved TiO_2/Fe_3O_4 recovery problem when it was used in the practical wastewater treatment factories. In additional, The prepared TiO_2/Fe_3O_4 photocatalyst was identified as anatase, and particle size was about 20~40 nm formed by XRD and FE-SEM. In the photodegradation experiments, the results indicated that 40~88% DRE reached at different amounts of TiO_2/Fe_3O_4, and the best addition amount was 5 g TiO_2/Fe_3O_4 under pH 10.

References

[1] T. C. Cheng, K. S. Yao, N. Yeh et al., "Bactericidal effect of blue LED light irradiated TiO_2/Fe_3O_4 particles on fish pathogen in seawater," *Thin Solid Films*, vol. 519, no. 15, pp. 5002–5006, 2011.

[2] Z. Zhang and J. Gamage, "Applications of photocatalytic disinfection," *International Journal of Photoenergy*, vol. 2010, Article ID 764870, 11 pages, 2010.

[3] C. Y. Chang, Y. H. Hsieh, L. L. Hsieh, K. S. Yao, and T. C. Cheng, "Establishment of activity indicator of TiO_2 photocatalytic reaction—hydroxyl radical trapping method," *Journal of Hazardous Materials*, vol. 166, no. 2-3, pp. 897–903, 2009.

[4] T. C. Cheng, K. S. Yao, Y. H. Hsieh, L. L. Hsieh, and C. Y. Chang, "Optimizing preparation of the TiO_2 thin film reactor using the Taguchi method," *Materials and Design*, vol. 31, no. 4, pp. 1749–1751, 2010.

[5] J. Anthony, P. A. Fernandez-Ibañez, P. S. M. Dunlop, D. M. A. Alrousan, and J. W. J. Hamilton, "Photocatalytic enhancement for solar disinfection of water: a review," *International Journal of Photoenergy*, vol. 2011, Article ID 798051, 12 pages, 2011.

[6] K. S. Yao, T. C. Cheng, S. J. Li et al., "Comparison of photocatalytic activities of various dye-modified TiO_2 thin films under visible light," *Surface and Coatings Technology*, vol. 203, no. 5–7, pp. 922–924, 2008.

[7] M. L. Chen and W. C. Oh, "The improved photocatalytic properties of methylene blue for V_2O_3/CNT/TiO_2 composite under visible light," *International Journal of Photoenergy*, vol. 2010, Article ID 264831, 6 pages, 2010.

[8] J. Yu, J. Xiong, B. Cheng, and S. Liu, "Fabrication and characterization of Ag-TiO_2 multiphase nanocomposite thin films with enhanced photocatalytic activity," *Applied Catalysis B*, vol. 60, no. 3-4, pp. 211–221, 2005.

[9] J. Zhou, Y. Cheng, and J. G. Yu, "Preparation and characterization of visible-light-driven plasmonic photocatalyst Ag/AgCl/TiO_2 nanocomposite thin films," *Journal of Photochemistry and Photobiology A*, vol. 223, no. 2-3, pp. 82–87, 2011.

[10] Y. Li, G. Lu, and S. Li, "Photocatalytic transformation of rhodamine B and its effect on hydrogen evolution over Pt/TiO_2 in the presence of electron donors," *Journal of Photochemistry and Photobiology A*, vol. 152, no. 1–3, pp. 219–228, 2002.

[11] J. Yu, Y. Hai, and B. Cheng, "Enhanced photocatalytic H_2-production activity of TiO_2 by $Ni(OH)_2$ cluster modification," *Journal of Physical Chemistry C*, vol. 115, no. 11, pp. 4953–4958, 2011.

[12] M. Zhou, J. Yu, S. Liu, P. Zhai, and L. Jiang, "Effects of calcination temperatures on photocatalytic activity of SnO_2/TiO_2 composite films prepared by an EPD method," *Journal of Hazardous Materials*, vol. 154, no. 1–3, pp. 1141–1148, 2008.

[13] G. Dai, J. Yu, and G. Liu, "Synthesis and enhanced visible-light photoelectrocatalytic activity of p-n junction BiOI/TiO_2 nanotube arrays," *Journal of Physical Chemistry C*, vol. 115, no. 15, pp. 7339–7346, 2011.

[14] S. M. Alves Jorge, J. J. de Sene, and A. de Oliveira Florentino, "Photoelectrocatalytic treatment of p-nitrophenol using Ti/TiO_2 thin-film electrode," *Journal of Photochemistry and Photobiology A*, vol. 174, no. 1, pp. 71–75, 2005.

[15] C. H. Shen, C. Y. Chang, and S. L. Lo, "Visible light activated photocatalytic degradation effect of V-TiO_2 on methyl tert-butyl ether," *Advanced Materials Research*, vol. 255-260, pp. 2705–2709, 2011.

[16] L. L. Hsieh, C. Y. Chang, H. L. Shyu, C. A. Tsou, and H. H. Lo, "The inhibition effect of TiO_2/Ag thin film on *Acinetobacter baumannii*," *Advanced Materials Research*, vol. 123-125, pp. 272–275, 2010.

[17] R. Poliah and S. Sreekantan, "Characterization and photocatalytic activity of enhanced Copper-Silica-loaded Titania prepared via hydrothermal method," *Journal of Nanomaterials*, vol. 2011, Article ID 239289, 8 pages, 2011.

[18] Y. Tian, D. Wu, X. Jia, B. Yu, and S. Zhan, "Core-shell nanostructure of α-Fe_2O_3/Fe_3O_4: synthesis and photocatalysis for methyl orange," *Journal of Nanomaterials*, vol. 2011, Article ID 837123, 5 pages, 2011.

[19] C. Y. Chang, Y. H. Hsieh, and Y. Y. Chen, "Photoelectrocatalytic degradation of sodium oxalate by TiO_2/Ti thin film electrode," *International Journal of Photoenergy*, vol. 2012, Article ID 576089, 6 pages, 2012.

[20] Q. Xiang, J. Yu, and M. Jaroniec, "Graphene-based semiconductor photocatalysts," *Chemical Society Reviews*, vol. 41, pp. 782–796, 2012.

[21] S. Liu, J. Yu, and M. Jaroniec, "Anatase TiO_2 with dominant high-energy 001 facets : synthesis, properties, and applications," *Chemistry of Materials*, vol. 23, pp. 4085–4093, 2011.

[22] X. Yu, S. Liu, and J. Yu, "Superparamagnetic γ-Fe_2O_3@SiO_2@TiO_2 composite microspheres with superior photocatalytic properties," *Applied Catalysis B*, vol. 104, no. 1-2, pp. 12–20, 2011.

[23] Y. J. Chang, J. W. Lee, C. H. Lin, C. Y. Chang, Y. C. Lee, and M. Y. Hwa, "Photocatalytic deactivation of airborne microbial cells by the stainless steel sieves with surface coated TiO_2 thin films," *Surface & Coatings Technology*, vol. 205, no. 1, pp. S328–S332, 2010.

[24] T. C. Cheng, K. S. Yao, N. Yeh et al., "Visible light activated bactericidal effect of TiO_2/Fe_3O_4 magnetic particles on fish pathogens," *Surface & Coatings Technology*, vol. 204, no. 6-7, pp. 1141–1144, 2009.

[25] M. Y. Chang, Y. H. Hsieh, T. C. Cheng, K. S. Yao, M. C. Wei, and C. Y. Chang, "Photocatalytic degradation of 2,4-dichlorophenol wastewater using porphyrin/TiO_2 complexes activated by visible light," *Thin Solid Films*, vol. 517, no. 14, pp. 3888–3891, 2009.

[26] L. Zhao, J. G. Ran, Z. Shu, G. T. Dai, P. G. Zhai, and S. M. Wang, "Effects of calcination temperatures on photocatalytic activity of ordered titanate nanoribbon/SnO2 films fabricated during an EPD process," *Journal of Photochemistry and Photobiology A*, vol. 2012, Article ID 472958, 7 pages, 2012.

[27] G. Shang, H. Fu, S. Yang, and T. Xu, "Mechanistic study of visible-light-induced photodegradation of 4-chlorophenol by TiO_{2-x} Nx with low nitrogen concentration," *International Journal of Photoenergy*, vol. 2012, Article ID 759306, 9 pages, 2012.

[28] J. Yu and J. Ran, "Facile preparation and enhanced photocatalytic H_2-production activity of $Cu(OH)_2$ cluster modified TiO_2," *Energy & Environmental Science*, vol. 4, no. 4, pp. 1364–1371, 2011.

[29] J. Yu and B. Wang, "Effect of calcination temperature on morphology and photoelectrochemical properties of anodized titanium dioxide nanotube arrays," *Applied Catalysis B*, vol. 94, no. 3-4, pp. 295–302, 2010.

[30] J. Yu, G. Dai, and B. Cheng, "Effect of crystallization methods on morphology and photocatalytic activity of anodized TiO_2 nanotube array films," *Journal of Physical Chemistry C*, vol. 114, no. 45, pp. 19378–19385, 2010.

[31] J. N. Zhang, *Introduction to Taguchi Quality Engineering*, Quality Control Society of the Republic of China, Taiwan, 1989.

[32] K. Y. Cheng, K. S. Yao, H. H. Lo, C. Y. Chang, and P. H. Chen, "Photoelectrocatalytic degradation of isopropyl alcohol by TiO_2/Ti thin-film electrode," *Advanced Materials Research*, vol. 123-125, pp. 165–168, 2010.